Journal for ImmunoTherapy of Cancer

Live attenuated bacterium limits cancer resistance to CAR-T therapy by remodeling the tumor microenvironment

Fengguang Guo [1], Jugal K Das,[1] Koichi S Kobayashi,[1,2] Qing-Ming Qin,[1] Thomas A Ficht,[3] Robert C Alaniz,[1] Jianxun Song [1], Paul De Figueiredo[1,3]

To cite: Guo F, Das JK, Kobayashi KS, *et al*. Live attenuated bacterium limits cancer resistance to CAR-T therapy by remodeling the tumor microenvironment. *Journal for ImmunoTherapy of Cancer* 2022;**10**:e003760. doi:10.1136/jitc-2021-003760

FG and JKD contributed equally.

Accepted 20 November 2021

[1]Department of Microbial Pathogenesis and Immunology, Texas A&M University Health Science Center, Bryan, TX 77802, USA
[2]Department of Immunology, Graduate School of Medicine, Hokkaido University, Sapporo 060-8638, Japan
[3]Department of Veterinary Pathobiology, College of Veterinary Medicine, Texas A&M University, College Station, TX 77843, USA

Correspondence to
Dr Paul De Figueiredo; pjdefigueiredo@tamu.edu

Dr Robert C Alaniz; robert_alaniz@tamu.edu

Dr Thomas A Ficht; tficht@tamu.edu

Dr Jianxun Song; jus35@tamu.edu

ABSTRACT

The tumor microenvironment (TME) is characterized by the activation of immune checkpoints, which limit the ability of immune cells to attack the growing cancer. To overcome immune suppression in the clinic, antigen-expressing viruses and bacteria have been developed to induce antitumor immunity. However, the safety and targeting specificity are the main concerns of using bacteria in clinical practice as antitumor agents. In our previous studies, we have developed an attenuated bacterial strain (*Brucella melitensis* 16M Δ*vjbR*, henceforth BmΔ*vjbR*) for clinical use, which is safe in all tested animal models and has been removed from the select agent list by the Centers for Disease Control and Prevention. In this study, we demonstrated that BmΔ*vjbR* homed to tumor tissue and improved the TME in a murine model of solid cancer. In addition, live BmΔ*vjbR* promoted proinflammatory M1 polarization of tumor macrophages and increased the number and activity of $CD8^+$ T cells in the tumor. In a murine colon adenocarcinoma model, when combined with adoptive transfer of tumor-specific carcinoembryonic antigen chimeric antigen receptor $CD8^+$ T cells, tumor cell growth and proliferation was almost completely abrogated, and host survival was 100%. Taken together, these findings demonstrate that the live attenuated bacterial treatment can defeat cancer resistance to chimeric antigen receptor T-cell therapy by remodeling the TME to promote macrophage and T cell-mediated antitumor immunity.

INTRODUCTION

In the tumor microenvironment (TME), cancer cells express factors to suppress immune surveillance, thereby creating a permissive environment for their uncontrolled proliferation.[1 2] The immunosuppressive TME is a key factor limiting the efficacy of chimeric antigen receptor T-cell (CAR-T) therapies, especially for solid tumors.[3] Several strategies are being developed to overcome TME-associated immunosuppression, including the activation of antitumor immunity by antigen-expressing viruses and bacteria.[4–6] However, improvements in the safety, targeting specificity, and efficacy of these agents are required for widespread adoption.[7] Here, we demonstrate that a safe, live attenuated bacterium (*Brucella melitensis* 16M Δ*vjbR*, henceforth BmΔ*vjbR*) homed to tumor tissue and improved the TME in a murine model of cancer. Moreover, we show that BmΔ*vjbR*, when paired with CAR-T therapy, displayed remarkable anticancer efficacy in this model.

BmΔ*vjbR* has been developed by our groups for clinical applications.[8 9] This strain is genetically and functionally defective in LuxR-type regulatory protein VjbR, which is required for expression of the bacterial type IV secretion system, an essential component of bacterial virulence.[10] A series of safety studies in immune-compromised mice and non-human primates showed that BmΔ*vjbR* does not induce disease-associated symptoms and resulted in removal of BmΔ*vjbR* from the select agent list by the Centers for Disease Control and Prevention.[8 11 12] Here, we show that BmΔ*vjbR* can remodel the TME to a proinflammatory state. Moreover, when BmΔ*vjbR* treatment was combined with the adoptive transfer of carcinoembryonic antigen CEA-Ag-specific $CD8^+$ T cells, tumor growth and proliferation were dramatically impaired.

MATERIALS AND METHODS

Bacterial culture and inoculation

Freshly cultured BmΔ*vjbR* in tryptone soya broth was collected by centrifugation and washed and resuspended in 1× phosphate-buffered saline (PBS, pH 7.4). For in vitro inoculation, bacteria were added in each well of a 24-well plate with macrophage monolayer at a multiplicity of infection (MOI) of 20 in Dulbecco's Modified Eagle's Medium (DMEM) (Thermo Fisher Scientific), and the plate was centrifuged at 500× g for 5 min to enhance bacterial interaction with the macrophages. After incubation at 37°C for 30 min to allow the macrophages to uptake the bacteria, the non-internalized bacteria were removed by washing the cell monolayer twice with warm PBS, and then fresh DMEM medium containing 50 µg/mL of gentamicin was added into each well for cell growth until assay. For in vivo animal experiment, at 9-day postinoculation of tumor cells in mice, 5×10^7 colony forming units (CFUs) of BmΔ*vjbR* in 100 µL of 1× PBS was intravenously injected into each mouse.

Macrophage cultures

For murine bone marrow-derived macrophage (BMDM) generation, bone marrow cells were harvested from the tibia and femur of C57BL/6 mice of 6–8 weeks and cultured as described previously.[13] Murine RAW264.7 (ATCC TIB-71) and J774A.1 (ATCC TIB-67) macrophage cell lines were both cultured in DMEM media containing 10% FBS and penicillin–streptomycin (100 IU/mL and 100 µg/mL).

Cytokine responses

BMDMs were seeded in 24-well plates at a concentration of 2.0×10^5 cells/well in DMEM without antibiotics. After overnight culture, the cells were inoculated with heat-killed (HK) or live BmΔ*vjbR* bacteria at a MOI of 20. At 24 hours post-treatment, cell culture supernatant was collected and analyzed for the presence of cytokines/chemokines by using a Multiplex Mouse Cytokine/Chemokine Array 31-Plex technology (MD31, Eve Technologies).

Flow cytometric analysis

$CD8^+$ T cells, isolated by using mouse $CD8^+$ T-cell isolation kit (BioLegend), were cocultured in vitro with BmΔ*vjbR*-treated macrophages. The $CD8^+$ T cells were then analyzed by flow cytometry following exclusion of dead cells by using Aqua Zombie NIR staining dye (BioLegend) and specific gating $CD8^+$ marker. The $CD8^+$ T-cell markers of programmed cell death protein 1 (PD-1), CD69, 4-1BB, CD27, CD62L, OX40, granzyme B (GrB), and perforin (Prf) were assessed either immediately after coculture with infected BMDMs or 3 days after re-stimulation with anti-CD3/CD28 antibodies. Intracellular cytokine staining was performed by using monensin and brefeldin (BioLegend) and the production of interleukin 2 (IL-2), tumor necrosis factor alpha (TNF-α), and interferon gamma (IFN-γ) was assessed. Similarly, the BMDMs were separately analyzed for the expression of CD38 on M1 macrophages. All flow cytometry data were acquired on a Fortessa X 20 (BD Biosciences, CA) and analyzed by using FlowJo (Treestar, OR).

CAR-T cell preparation

The MSGV1 γ retroviral vector backbone was modified to express CEA specific scFv, as described in our previous study.[14] Briefly, $CD8^+$ T cells isolated from B6 Thy 1.2 mice were transduced with the viral supernatants containing CEA in the presence of 5 µg/mL Polybrene (Sigma Aldrich, USA), following a protocol as described previously.[15] The transduced cells were positively identified by expression of c-Myc.

Animal experimentation

The wild-type C57BL/6 (B6) Thy 1.1 mice (Jackson Laboratories) 6–8 weeks old were subcutaneously injected with 1×10^6 MC32 CEA cancer cells in the right lateral flank on day 0. Subsequently, the mice were divided into three different groups (n=5) with each group receiving either 1× PBS control (Ctrl), HK bacteria or live attenuated bacteria (Live) on day 9 postinoculation of tumor cells. On day 12 postinduction of the tumor, all the groups of mice received the CEA CAR-Ts isolated and prepared from Thy 1.2 mice 6–8 weeks old. Mice were housed in Texas A&M University, Laboratory Animal Resources and Research Facility, and checked daily. Tumor growth was monitored every other day and tumor volumes were calculated using the formula: Tumor Volume (mm^3)=0.5 × length × $width^2$. Mice were humanely sacrificed if tumor size reached above 4000 mm3.

Fluorescence imaging of BmΔ*vjbR*

Formaldehyde fixed tissue or macrophage monolayer were used for BmΔ*vjbR* staining. For staining bacteria in tumor tissue, formalin fixed, paraffin-embedded sections of MC32 tumor tissue were deparaffinized in xylene and rehydrated through graded alcohols, and then antigen was retrieved in a pressure cooker using a citrate buffer. The cells were stained with rabbit anti-*Brucella* antibodies (Bioss Inc.) for 1 hour followed by appropriate secondary antibody for 1 hour. Cells were mounted with ProLong Glass Antifade Mountant with NucBlue Stain (Thermo Fisher Scientific). All the images were acquired using a Nikon Eclipse Ti2 fluorescence microscope.

Bacterial quantification

For detecting BmΔ*vjbR* survival in BMDMs, J774A.1 or RAW 264.7 cell lines, cells were seeded in a 24-well plate in 1 mL of DMEM without antibiotics at 2.0×10^5 cells/well. The CFU of bacteria at different postinoculation times was assayed by spotting serial dilution on tryptone soya agar (TSA) plates. For CFU assay of BmΔ*vjbR* in different organs of cancer bearing mice, the organ-homogenates were obtained 19 days postinoculation and spotted on TSA plates for enumeration of bacteria.

Comparative metabolic analysis

The differences in the glycolytic states of $CD8^+$ T cells were analyzed using extracellular flux (XF) analyzers (Agilent) using a protocol described previously.[16] Briefly, after coculture with BmΔ*vjbR* infected BMDMs for 16 hours, T cells in suspension were removed from the cocultured medium and seeded on 96-well seahorse plates. Their XF and compensatory glycolysis were assessed by using glycolytic activators and inhibitors as described in the Seahorse XF protocol.

Imaging and immunohistochemistry of tumor sections

Paraffin-embedded solid tumor samples were sliced into 5 µm sections with microtome. The slides that were prepared from these sections were processed for fluorescence

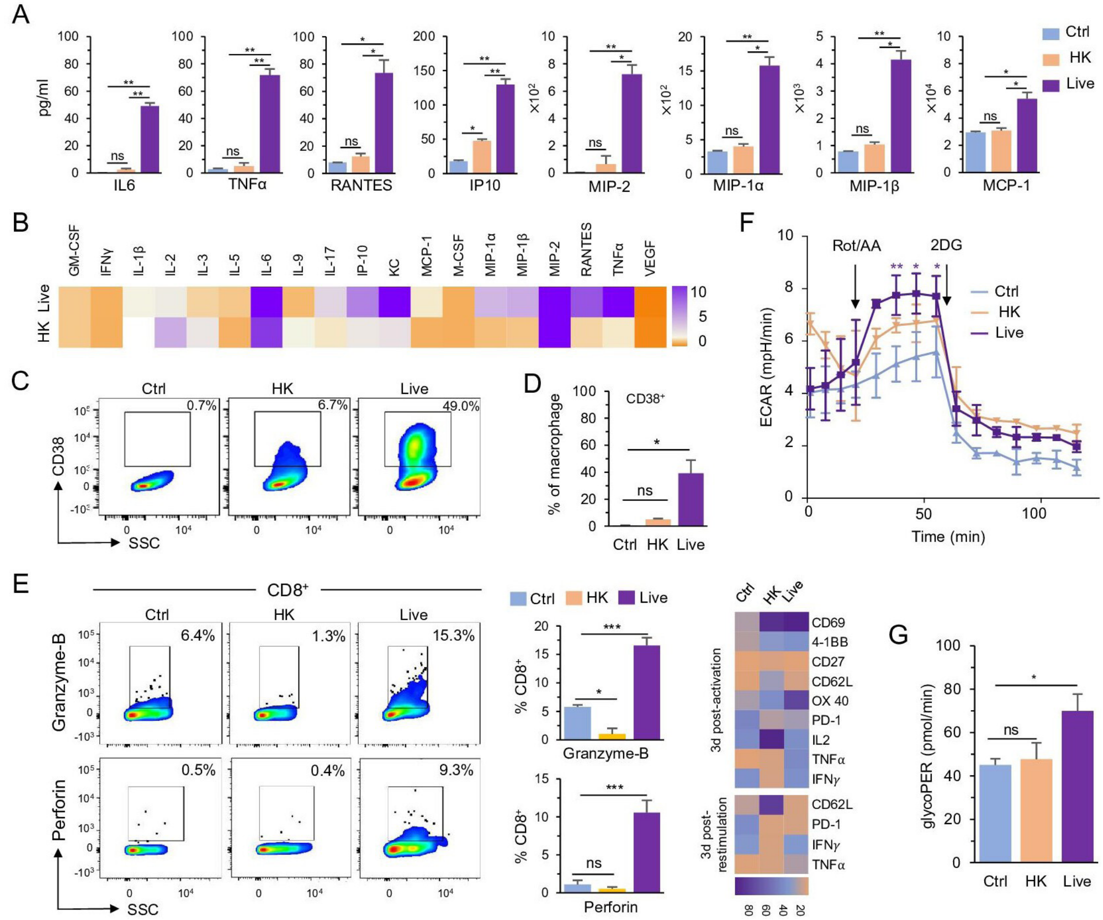

Figure 1 Live BmΔ*vjbR* treatment activates CD8⁺ T cells to produce proinflammatory cytokines by polarizing macrophages. (A,B) Cytokine array analysis of the culture medium of BMDMs after treatment with 1× PBS (Ctrl), HK or live) BmΔ*vjbR* for 24 hours shown live BmΔ*vjbR* promotes BMDMs to secret proinflammatory cytokines and chemokines. (C,D) Flowcytometric analysis of CD38 expression on BMDMs after treatment with HK or live BmΔ*vjbR* for 24 hours. (E) Coculturing with live BmΔ*vjbR*-infected BMDMs activates CD8⁺ T cells to produce granzyme B and perforin (left) and express activation markers and cytokines (right heatmap). (F,G) Cocultivation with live BmΔ*vjbR*-infected BMDMs increases the glycolysis of CD8⁺ T cells. Data represent means±SD from three independent experiments. *, **, ***Significance at p<0.05, 0.01, and 0.001, respectively. BMDM, bone marrow-derived macrophage; Ctrl, control; ECAR, extracellular acidification rate; GM-CSF, granulocyte-macrophage colony-stimulating factor;HK, heat-killed; IFN-γ, interferon gamma; IL, interleukin; IP-10, interferon gamma-induced protein 10; KC, keratinocytes-derived chemokine; MCP-1, monocyte chemoattractant protein 1; M-CSF, macrophage colony-stimulating factor; MIP, macrophage inflammatory protein; ns, not significant; RANTES, chemokine (C-C motif) ligand 5; VEGF, vascular endothelial growth factor; PBS, phosphate-buffered saline; SSC, side scatter; TNF-α, tumor necrosis factor alpha.

microscopy, H&E staining, and mass cytometry analysis. The H&E stained slides were scored for inhibition of tumor by assessing the necrotic areas and infiltration of immune cells on a scale of 1–5. The score was represented as tumor inhibition score in the comparative bar–graph analysis.

Imaging mass cytometry (IMC) analysis

IMC analysis of tumor samples derived from BmΔ*vjbR* treated mice or PBS controls were processed for the quantification, imaging, and analysis of DNA, Ki67 antigen, CD8⁺ T cells, B220 (B cells), CD11c (dendritic cells), and F4/80 (macrophages) respectively. A dimensionality reduction technique was adopted to construct t-distributed stochastic neighbor embedding (t-SNE) plots from the heatmaps of treated or untreated groups of mice. The neighborhood analysis was constructed to find the probability of enriched cell-to-cell interactions using basic statistical methods as described previously.[17]

Statistical analysis

All analyses were performed using Graphpad Prism V.9. Unpaired t-test was performed to compare the difference between the groups. A p value of <0.05 was considered statistically significant.

RESULTS

Live BmΔ*vjbR* induces anticancer phenotypes in BMDMs and CD8⁺ T cells

To test the hypothesis that BmΔ*vjbR* elicits anti-cancer proinflammatory phenotypes from immune cells, we incubated the live attenuated strain with murine BMDMs

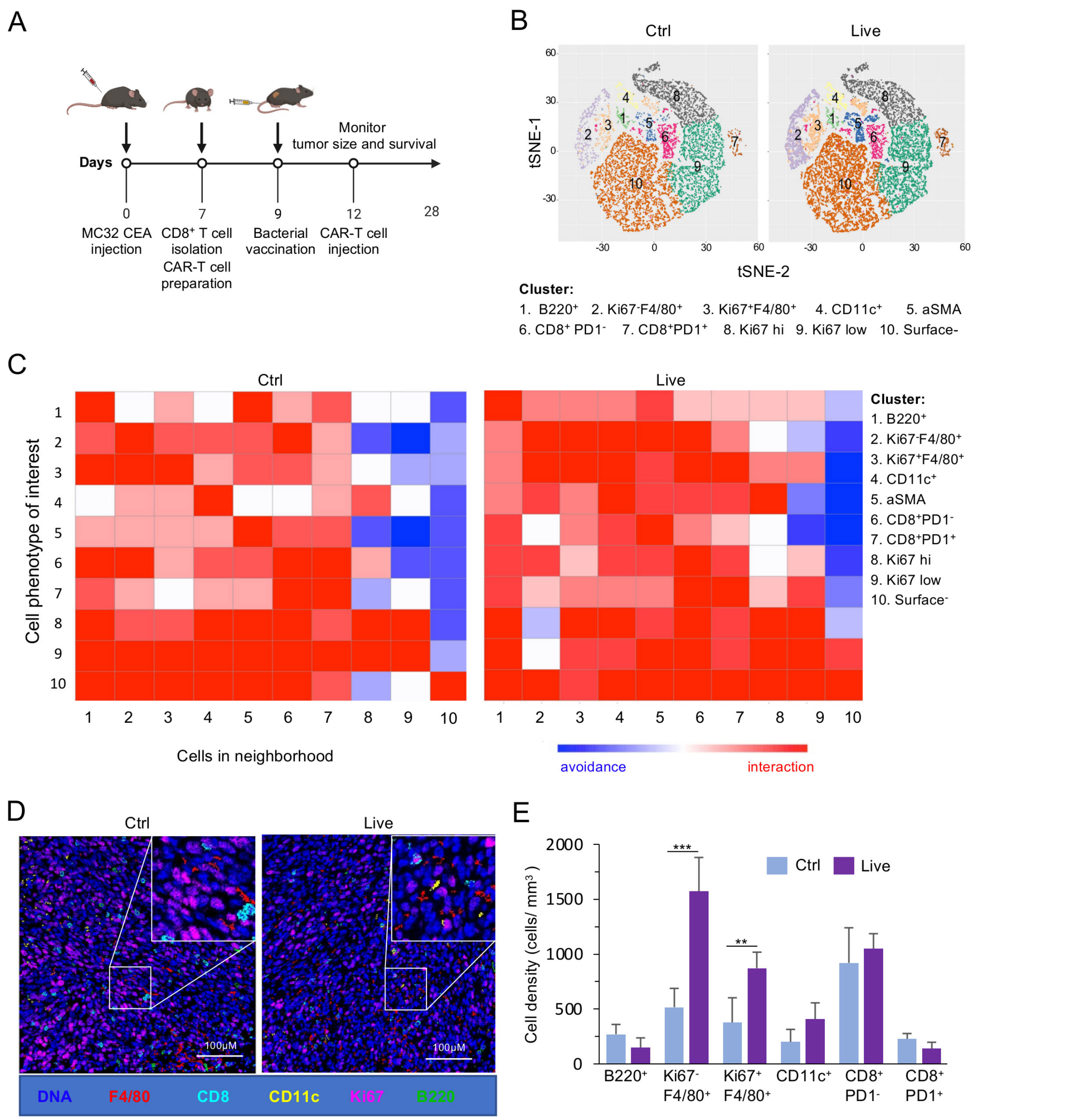

Figure 2 Live BmΔ*vjbR*-treated mice show a significant increase in innate immune cells. Mass cytometry analysis of MC32 CEA derived tumor samples (three samples/group) from Thy 1.1 mice either intravenously injected with live BmΔ*vjbR* or 1× PBS (Ctrl) prior to intravenous administration of CEA CAR-Ts. (A) Schematic diagram showing adoptive T-cell therapy and BmΔ*vjbR* treatment protocol. (B) Visualization of t-distributed stochastic neighbor embedding (viSNE) plots of comparative immune cell populations in the Ctrl and live BmΔ*vjbR* treated tumor samples. (C) Neighborhood joining plots of different immune cell populations in tumor tissues with highly interacting neighbored cells shown in red, whereas the avoided interactions are shown in blue. (D) Reconstructed image of immune cell infiltration into tumor samples. (E) Quantification of macrophages, dendritic cells, and B cells in tumor samples (three fields/sample were analyzed). **, ***Significance at p< 0.01 and 0.001, respectively. The markers representing the different immune cell populations are B220 (B cells), F4/80 (macrophages), CD11c (dendritic cells), Ki67 (proliferating cells), $CD8^+$ ($CD8^+$ T cells) and $surface^-$ (cells are negative to all tested makers). CAR-T, chimeric antigen receptor T cell; CEA, carcinoembryonic antigen; Ctrl, control; PBS, phosphate-buffered saline.

for 24 hours, and then measured cytokine secretion and macrophage polarization. We found that, in contrast to HK or no-treatment Ctrl, live BmΔ*vjbR* (Live) enhanced the secretion of proinflammatory cytokines and chemokines (figure 1A,B). Most of these BMDMs were polarized to M1 macrophages, which express CD38, an M1 exclusive marker, on their surface (figure 1C,D). Collectively, these data suggested that live BmΔ*vjbR* activates macrophages and induces the production of proinflammatory cytokines and T cell-mediated chemo-attractants.[18 19]

After coculturing $CD8^+$ T cells with BMDMs pre-treated with either live or HK bacteria, we found that BMDMs exposed to live BmΔ*vjbR* activated $CD8^+$ T cells more efficiently compared with HK controls through upregulating

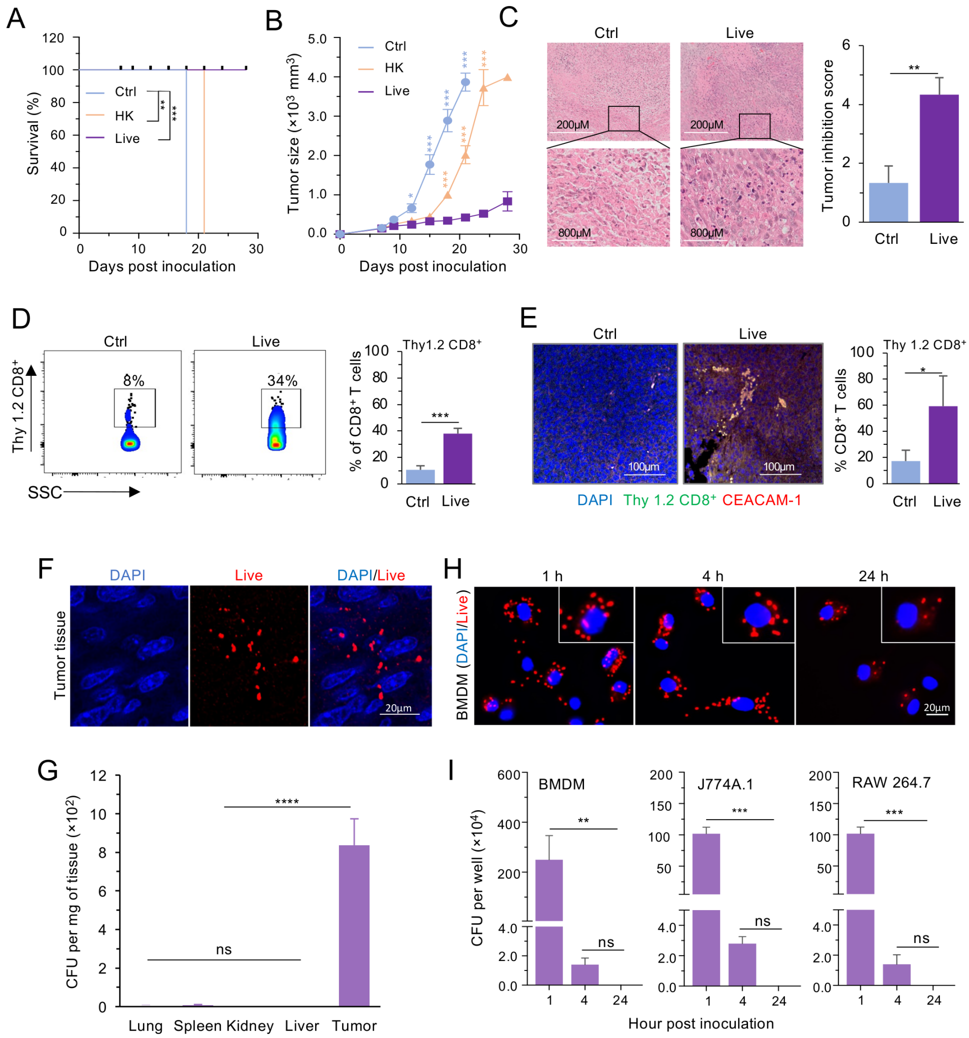

Figure 3 BmΔ*vjbR* accumulates in tumor tissue and suppresses tumor growth. Three groups of MC32 tumor-bearing C57BL/6 (B6) mice (five mice/group) were intravenously injected with either live, HK BmΔ*vjbR*, or 1× PBS (Ctrl). On day 3 postbacteria treatment, all three groups of mice were intravenously injected with CEA CAR-Ts. (A) Survival of mice is significantly improved in the group receiving BmΔ*vjbR* from 18 days onwards compared with the control untreated group (n=5 mice/group). (B) Live BmΔ*vjbR* immunization followed by adoptive T-cell transfer significantly suppresses the tumor growth from 18 days postinitiation of the experiment compared with both non-bacterial (Ctrl) and HK BmΔ*vjbR* (HK) treatment groups (n=5 mice/group). (C) H&E staining shows significant improvement in tumor in the group of mice receiving BmΔ*vjbR* compared with the Ctrl group. (D,E) Flow cytometry (D) and confocal microscopy (E) followed by graphical representation of infiltrating lymphocytes (Thy 1.2 CD8$^+$ T cells) confirm significantly higher infiltration of adoptively transferred CEA CD8$^+$ T cells. (F) Representative immunofluorescence microscopy images show BmΔ*vjbR* survival in tumor tissue 19 days postinjection. (G) BmΔ*vjbR* mainly colonizes in tumor (n=3). (H) BmΔ*vjbR* can be observed in BMDMs with immunofluorescence microscopy after 1, 4, and 24 hpi. (I) The BmΔ*vjbR* can be recovered from BMDMs, J774A.1, and RAW 264.7 macrophages at 1 hpi and four hpi, but no bacteria survived in these macrophages at 24 hpi. Three independent experiments were performed for H and I. Data represent means±SD. *, **, ***, ****Significance at p<0.05, 0.01, 0.001, and 0.0001, respectively. BMDM, bone marrow derived macrophage; CFU, colony forming unit; CAR-T, chimeric antigen receptor T cell; Ctrl, control; DAPI, 4′,6-diamidino-2-phenylindole; HK, heat-killed; hpi, hours postinoculation; ns, not significant; PBS, phosphate-buffered saline.

the expression of GrB and Prf (figure 1E, left). The live BmΔ*vjbR*-treated BMDMs also induced significantly higher production of TNF-α, IFN-γ, and IL-2 from CD8$^+$ T cells (figure 1E, right top). Moreover, costimulatory marker expression, including OX40 and 4-1BB, was higher in CD8$^+$ T cells cocultured with BmΔ*vjbR*-treated BMDMs (figure 1E, right top). To test the hypothesis that the activated CD8$^+$ T cells retained functional recall ability, a feature critical for antitumor efficacy,[20] we used anti-CD3/anti-CD28 antibodies to restimulate CD8$^+$ T cells at 3-day postactivation. We found that the CD8$^+$ T-cell recall responses were enhanced post-restimulation, exhibiting lower PD-1 expression and higher expression of proinflammatory cytokines (figure 1E, right bottom). CD8$^+$ T cells also had a significantly higher extracellular acidification rate and showed higher glycolytic activity when activated with BMDMs treated with live BmΔ*vjbR* (figure 1F,G).

BmΔ*vjbR* induces diverse cellular responses

We hypothesized that BmΔ*vjbR* treatment may alter the TME in an in vivo murine solid-tumor system. To test this hypothesis, we performed an IMC analysis to quantify the abundance of B cells as well as proliferating and non-proliferating immune cells from explanted solid tumors. A well-established MC32 colon cancer murine model was used for the experiment, following the protocol shown in figure 2A. We found that live BmΔ*vjbR*-treated mice had a higher complexity of immune cells in the TME (figure 2B,C) compared with controls. To determine the identities of enriched interactions between or within the cell phenotypes in the TME, we constructed neighborhood joining plots from the IMC data. The t-distributed stochastic neighbor embedding (t-SNE) plots (figure 2B) and neighborhood joining analysis (figure 2C) showed that innate immune cells were activated and quantitatively higher in the TME of mice receiving the treatment. The reconstructed image from the mass cytometry analysis showed more immune cells, especially $F4/80^+$ macrophages, in the TME of BmΔ*vjbR* treated mice receiving adoptive transfer of CAR-Ts (figure 2D). Therefore, we quantified the specific innate immune cells from the TME and found that the numbers of $Ki67^-F4/80^+$ (non-proliferating macrophages) and $Ki67^+F4/80^+$ (proliferating macrophages) were significantly increased in BmΔ*vjbR*-treated mice receiving adoptive transfer of CAR-Ts (figure 2E). Overall, our results indicated that the numbers of macrophages and dendritic cells were significantly increased in the TME of treated mice receiving adoptive transfer of CAR-Ts, consistent with the hypothesis that these immune cells promote CAR-T tumor infiltration and drive tumor regression.

BmΔ*vjbR* treatment enhances antitumor efficacy and selectively colonizes tumor tissue

Encouraged by our findings, we tested the hypothesis that BmΔ*vjbR* treatment enhances the antitumor efficacy of CAR-T therapy. We found that BmΔ*vjbR*-treated mice displayed significantly greater survival (figure 3A) and had drastically lower tumor burden than controls (figure 3B,C). We found that there were significantly increased numbers of $CD8^+$ T cells infiltrating into the solid tumor of mice that were treated with live BmΔ*vjbR*, in comparison to control (figure 3D,E).

We also measured BmΔ*vjbR* clearance from treated mice. Nineteen days after intravenous injection, we found BmΔ*vjbR* in tumor tissue (figure 3F) but not in other organs (figure 3G). We also monitored the survival of BmΔ*vjbR* in macrophages in vitro using immunofluorescence staining and CFU enumeration. We found numerous bacterial cells in BMDMs at 1 and 4 hours postinoculation (hpi). However, fewer were observed at 24 hpi (figure 3H). Importantly, live bacteria were only recovered from BMDMs at 1 and 4 hpi, and no bacteria survived longer than 24 hpi in BMDMs, J774A.1, and RAW 264.7 (figure 3I). These results indicate the BmΔ*vjbR* strain selectively targeted the tumor, survived for only short times in macrophages and were rapidly cleared from non-tumor tissue after treatment.

DISCUSSION

Cancer cells suppress immune surveillance, thereby creating a permissive environment for cancer cell proliferation. In this work, we show that a novel and safe live attenuated bacterial strain BmΔ*vjbR* can remodel the TME to a proinflammatory status and thereby limit cancer progression and tumorigenesis. Moreover, we have shown that BmΔ*vjbR* treatment, when combined with the adoptive transfer of antigen-specific $CD8^+$ T cells, results in dramatically impaired tumor growth and proliferation. Therefore, this live attenuated bacterial strain potentiates immune surveillance and control of cancer.

Previous studies have demonstrated that treatment with live attenuated bacteria can limit tumorigenesis by a variety of mechanisms, such as activating T cells and expressing tumor antigens.[6 21 22] Even though some of these bacterial approaches have entered clinical trials,[23 24] most previously used bacterial vectors have intrinsic deleterious or toxic features, and suboptimal safety profiles or routes of delivery that may significantly limit their broad utility in cancer therapy/treatment. Among the negative features observed are intraperitoneal route of delivery,[25] significant endotoxin activity, pathogenic reversion potential and limitations due to pre-existing host immunity.[26 27] So far, we have no evidence to suggest that BmΔ*vjbR* possesses the common deleterious properties shared by many of the previously studied bacterial vectors.[28] Moreover, this work provides the first description of combining live attenuated bacterium treatment with CAR-T therapy and thereby demonstrates the synergy that can be achieved with these approaches.

Acknowledgements We thank Robbie Moore from the College of Medicine Cell Analysis Facility, Malea Murphy from the Integrated Microscopy and Imaging Laboratory, Sankar P Chaki from the College of Veterinary Medicine, and Elizabeth Bustamante and Julia Plocica from Health Science Center at Texas A&M University, and the Immunomonitoring Core facility at Houston Methodist Hospital-Texas Medical Center for their technical support.

Contributors FG, JKD, PDF, JS, RCA, and TAF conceived and designed the experiments. FG and JKD performed the experiments and analyzed the data. PDF, JS, FG, JKD, RCA, TAF, Q-MQ, and KSK wrote the manuscript and provided critical feedback. PDF and JS supervised the research. All the authors read and approved the final manuscript.

Funding This work was supported by funding from the National Institutes of Health (R01AI121180 and R01CA221867 to JS, R01AI110642 to RCA, R01HD084339 to TAF, and R01AI141607-01A1 to PDF, NSF DBI1532188, and NSF0854684 to PDF).

Competing interests No, there are no competing interests.

Patient consent for publication Not applicable.

Ethics approval This study does not involve human subjects. All experiments were approved and performed in compliance with the regulations of The Texas A&M University Animal Care Committee (Institutional Animal Care & Use Committee, #2018–0065) and in accordance with the guidelines of the Association for the Assessment and Accreditation of Laboratory Animal Care.

Provenance and peer review Not commissioned; externally peer reviewed.

Data availability statement Data are available upon reasonable request. All data relevant to the study are included in the article or uploaded as supplementary information. The data presented in this report are available from the corresponding author on reasonable request.

ORCID iDs
Fengguang Guo http://orcid.org/0000-0002-3742-7214
Jianxun Song http://orcid.org/0000-0002-9734-6176

REFERENCES

1 Quail DF, Joyce JA. Microenvironmental regulation of tumor progression and metastasis. *Nat Med* 2013;19:1423–37.
2 Fridman WH, Pagès F, Sautès-Fridman C, *et al*. The immune contexture in human tumours: impact on clinical outcome. *Nat Rev Cancer* 2012;12:298–306.
3 Giraldo NA, Sanchez-Salas R, Peske JD, *et al*. The clinical role of the Tme in solid cancer. *Br J Cancer* 2019;120:45–53.
4 Nishikawa H, Sato E, Briones G, *et al*. In vivo antigen delivery by a Salmonella typhimurium type III secretion system for therapeutic cancer vaccines. *J Clin Invest* 2006;116:1946–54.
5 Quispe-Tintaya W, Chandra D, Jahangir A, *et al*. Nontoxic radioactive Listeria(at) is a highly effective therapy against metastatic pancreatic cancer. *Proc Natl Acad Sci U S A* 2013;110:8668–73.
6 Selvanesan BC, Chandra D, Quispe-Tintaya W. Tumor-targeted delivery of childhood vaccine recall antigens by attenuated Listeria reduces pancreatic cancer. *bioRxiv* 2021.
7 Forbes NS. Engineering the perfect (bacterial) cancer therapy. *Nat Rev Cancer* 2010;10:785–94.
8 Arenas-Gamboa AM, Rice-Ficht AC, Fan Y, *et al*. Extended safety and efficacy studies of the attenuated Brucella vaccine candidates 16 M(Delta)vjbR and S19(Delta)vjbR in the immunocompromised IRF-1-/- mouse model. *Clin Vaccine Immunol* 2012;19:249–60.
9 de Figueiredo P, Ficht TA, Rice-Ficht A, *et al*. Pathogenesis and immunobiology of brucellosis: review of Brucella-host interactions. *Am J Pathol* 2015;185:1505–17.
10 Delrue R-M, Deschamps C, Léonard S, *et al*. A quorum-sensing regulator controls expression of both the type IV secretion system and the flagellar apparatus of Brucella melitensis. *Cell Microbiol* 2005;7:1151–61.
11 Lee KM, Chiu KB, Sansing HA, *et al*. Aerosol-induced brucellosis increases TLR-2 expression and increased complexity in the microanatomy of astroglia in rhesus macaques. *Front Cell Infect Microbiol* 2013;3:86.
12 CDC. 2014 attenuated strains of overlap select agents excluded from the requirements of 9 cfr part 121 and 42 cfr part 73, 2014. Available: https://www.cdc.gov/selectagent/exclusions-overlap.html
13 Eshghjoo S, Kim DM, Jayaraman A, *et al*. A comprehensive high-efficiency protocol for isolation, culture, polarization, and glycolytic characterization of bone marrow-derived macrophages. *JoVE* 2021.
14 Fan J, Das JK, Xiong X, *et al*. Development of CAR-T cell persistence in adoptive immunotherapy of solid tumors. *Front Oncol* 2020;10:574860.
15 Song J, So T, Cheng M, *et al*. Sustained survivin expression from OX40 costimulatory signals drives T cell clonal expansion. *Immunity* 2005;22:621–31.
16 Eshghjoo S, Kim DM, Jayaraman A, *et al*. A comprehensive high-efficiency protocol for isolation, culture, polarization, and glycolytic characterization of bone marrow-derived macrophages. *J Vis Exp* 2021:e61959.
17 Schapiro D, Jackson HW, Raghuraman S, *et al*. histoCAT: analysis of cell phenotypes and interactions in multiplex image cytometry data. *Nat Methods* 2017;14:873–6.
18 Pathria P, Louis TL, Varner JA. Targeting tumor-associated macrophages in cancer. *Trends Immunol* 2019;40:310–27.
19 Liu J, Li F, Ping Y, *et al*. Local production of the chemokines CCL5 and CXCL10 attracts CD8+ T lymphocytes into esophageal squamous cell carcinoma. *Oncotarget* 2015;6:24978–89.
20 Liikanen I, Lauhan C, Quon S, *et al*. Hypoxia-Inducible factor activity promotes antitumor effector function and tissue residency by CD8+ T cells. *J Clin Invest* 2021;131. doi:10.1172/JCI143729. [Epub ahead of print: 01 04 2021].
21 Kim SH, Castro F, Paterson Y, *et al*. High efficacy of a Listeria-based vaccine against metastatic breast cancer reveals a dual mode of action. *Cancer Res* 2009;69:5860–6.
22 Chandra D, Quispe-Tintaya W, Jahangir A, *et al*. STING ligand c-di-GMP improves cancer vaccination against metastatic breast cancer. *Cancer Immunol Res* 2014;2:901–10.
23 Toso JF, Gill VJ, Hwu P, *et al*. Phase I study of the intravenous administration of attenuated Salmonella typhimurium to patients with metastatic melanoma. *J Clin Oncol* 2002;20:142–52.
24 Hassan R, Alley E, Kindler H, *et al*. Clinical Response of Live-Attenuated, *Listeria monocytogenes* Expressing Mesothelin (CRS-207) with Chemotherapy in Patients with Malignant Pleural Mesothelioma. *Clin Cancer Res* 2019;25:5787–98.
25 Zhang Y, Tome Y, Suetsugu A, *et al*. Determination of the optimal route of administration of Salmonella typhimurium A1-R to target breast cancer in nude mice. *Anticancer Res* 2012;32:2501–8.
26 Goldszmid RS, Dzutsev A, Trinchieri G. Host immune response to infection and cancer: unexpected commonalities. *Cell Host Microbe* 2014;15:295–305.
27 Zhang Z, Tang H, Chen P, *et al*. Demystifying the manipulation of host immunity, metabolism, and extraintestinal tumors by the gut microbiome. *Signal Transduct Target Ther* 2019;4:41.
28 Forbes NS, Munn LL, Fukumura D, *et al*. Sparse initial entrapment of systemically injected Salmonella typhimurium leads to heterogeneous accumulation within tumors. *Cancer Res* 2003;63:5188–93.